Numerical studies of the spectrum of low-intensity ultrasound scattered by bubbles

Brian C. Eatock and Ronald Y. Nishi
Defence and Civil Institute of Environmental Medicine, 1133 Sheppard Avenue West, P.O. Box 2000, Downsview, Ontario, Canada M3M 3B9

Gordon W. Johnston
University of Toronto Institute for Aerospace Studies, 4925 Dufferin Street, Downsview, Ontario, Canada M3H 5T6

(Received 28 May 1984; accepted for publication 16 January 1985)

The magnitude of the nonlinear effect in the scattering of ultrasound by nitrogen bubbles in water is examined numerically, for ultrasonic frequencies and amplitudes typical of diagnostic medical devices, to determine the suitability of this effect for the detection of bubbles in blood or tissue for application in decompression research. Numerical solutions of the modified "Rayleigh" equation, including the effects of acoustic, thermal, and viscous damping, and the dependence of the polytropic exponent on frequency are presented for pulsed ultrasound. For the chosen conditions, it is shown that nonlinear scattering is significant only for the population of bubbles which are smaller than, or close to, resonance size, and primarily for those bubbles that are one-half resonance size.

PACS numbers: 43.25.Yw, 43.80.Sh

INTRODUCTION

A. Description of the problem

There is a continuing need for information about gas bubbles which form in persons who are exposed to large reductions in ambient pressure. Three occupational groups routinely experience such pressure reductions: divers,[1] caisson workers,[2] and aviators.[3] During decompression, or up to several hours afterward, decompression sickness may develop, with consequences ranging from mild pain to disorders of the central nervous system.[1] Over the long term, the cumulative effects of decompression may lead to damage such as dysbaric osteonecrosis.[4]

Ultrasonic methods have been employed for the detection of decompression bubbles in man and animals since 1963.[5] Currently, of the several techniques available, the most widely used[5,6] relies on detection of the Doppler shifted component of the ultrasound scattered by moving targets in the blood. Use of the Doppler signal eliminates the large masking signal from stationary tissue, and reduces low-frequency artifacts caused by probe movement. The operator listens to the Doppler signal, which typically includes contributions from the heart wall, valves, and blood flow. Bubbles are identified by their transient, irregular sounds. This technique has the following limitations: it requires trained and vigilant monitors; it is subjective; and it detects only moving, intravascular bubbles.[7] Pulsed ultrasonic imaging (*B*-scan) is the second technique currently used for bubble detection.[8,9] With it, stationary bubbles which are trapped in tissue can be located. Such bubbles are thought to be the cause of decompression sickness. It is, however, not practical to map the whole body, and, furthermore, this technique is more complex, costly, and difficult to apply. Consequently, it is not used as widely as the Doppler method. Except in well-controlled *in vitro* experiments, it is not possible to obtain a measurement of the size of the bubbles from the amplitude of the scattered ultrasound with either of these techniques.[10] Bubbles as small as 5 μm in radius have been detected *in vitro*,[11,12] but the competition from background scatterers, such as erythrocytes, would increase this threshold by at least an order of magnitude *in vivo*.[13]

With either of the current methods, the bubble signal is masked by the signal from scatterers which are not of interest. This masking limits the sensitivity of the technique. An alternative method was proposed by Tucker and Welsby,[14] and Welsby and Safar,[15] based on monitoring the second harmonic of the ultrasound produced by nonlinear oscillations of the bubbles. This method would not suffer from the same limitations because only the bubbles would contribute significantly to the second harmonic signal.

B. Literature review

Preliminary experiments to test the proposed method were reported by Evans,[5] who worked in cooperation with Welsby. *In vitro* tests using clouds of bubbles were promising, but *in vivo* tests were inconclusive. Martin *et al.*[16] also tested the idea, both *in vitro*, and using human subjects, who were monitored during decompression from simulated dives. Their results were also promising, but the technique appears not to have been further developed by them. Moulinier[17] described in detail an instrument designed to detect bubbles in tissue using this method. He described a number of *in vitro* tests using bubbles produced by decompression or by electrolysis, and *in vivo* tests with a rabbit. The results obtained with his instrument were compared with indications provided by a Doppler bubble detector. The results

were generally positive, but Moulinier concluded that further tests and development were necessary. Recently, Miller[18,19] has reported the use of this technique to detect, specifically, bubbles resonant at the ultrasonic frequency of the instrument. The application in his case was to indicate the formation of bubbles by cavitation, rather than by decompression.

The numerical investigations described here were carried out in order to predict the magnitude of the nonlinear effect in the scattering of ultrasound by bubbles, for ultrasonic amplitudes and frequencies representative of those which might be considered for detection of bubbles in animals and man. A previous analytical study by Storm[20] addressed a similar problem, but used different techniques and had a different emphasis. The results of the two studies are complementary.

The model of bubble oscillations used was the familiar "Rayleigh model,"[21] so-called for simplicity, although it owes its present form to the contributions of several authors.[22–24] Lauterborn[25] made extensive numerical calculations with this model in order to explore the nonlinear behavior of small gas bubbles (0.1, 1.0, and 10.0 μm) in an ultrasonic field. He was particularly interested in elucidating the occurrence of subharmonics.

The equation which Lauterborn used[25] included only viscous damping, as derived by Poritsky,[24] because viscosity is the dominant damping mechanism for very small bubbles. The other damping mechanisms are acoustic damping, for which an analytical expression exists,[26,27] and thermal damping, which exhibits a complex dependence on bubble size and ultrasonic frequency.[28,29] Other expressions for the thermal damping coefficient were derived for resonant bubble oscillations.[30–34] These expressions were based on linearized models of spherical bubble oscillations. More advanced nonlinear models, which consider the compressibility of the liquid, include the damping of oscillations by radiation of sound inherently.[31,35,36]

Nishi[34] investigated absorption and scattering of ultrasound by bubbles with a linear theory which included heat exchange between the bubble and liquid, viscosity of the liquid and gas, and acoustic radiation. He considered factors pertinent to the decompression bubble detection problem. For example, he compared results for water with those for blood, which has a higher viscosity, for various hydrostatic pressures from 1 to 10 bars. A general linear solution to the problem of scattering of waves by cavities in viscoelastic media has been reported by Gaunaurd *et al.*[37] and Gaunaurd and Überall.[38]

Zabolotskaya and Soluyan,[39] Prosperetti,[40,41] and Storm[20] have reported analytical investigations of the nonlinear problem, but their solutions were not applicable to all cases of interest for bubble detection *in vivo*. In addition, a comparison of analytical results with numerical results seemed useful. Therefore, the numerical approach was chosen.

Because the literature of bubble dynamics is large, only papers which have had a direct bearing on this work have been cited. The literature has been reviewed by Plesset and Prosperetti,[42] Kapustina,[32] and Flynn.[31]

C. Scope of the investigation

The scope of this investigation has been limited to conditions which might be practical for ultrasonic bubble detection in man and animals. Therefore the ultrasonic intensities chosen for study were generally low (10–100 mW cm^{-2}). Higher intensities might cause ultrasonic cavitation in the (possibly) supersaturated blood or tissue of the subject; information on the cavitation thresholds for these conditions is lacking. The frequencies chosen ranged primarily from 100 kHz to 1 MHz. The higher frequency is more representative of medical ultrasonics, and is more convenient to use in practice, but lower frequencies may be more important for bubble detection. Bubble size in tissue may vary from a few micrometers to a several hundred micrometers in radius. Most of the numerical results were obtained for bubbles 1–20 μm in radius.

I. THEORY

The "Rayleigh" model of a gas bubble was the basis for this work. In this model, the bubble is considered to be spherical and surrounded by an incompressible liquid of infinite extent. Only radial motion is considered. A sinusoidal, time-varying pressure is applied uniformly over the bubble surface. This model assumes that the wavelength of the ultrasound is much greater than the radius of the bubble, and that only the behavior of the bubble surface is of interest. Gravity is not considered, but viscosity of the liquid is included. Although a real bubble in blood or tissue would not be subject to these constraints, nevertheless, this simple model may still provide useful information.

The equation solved numerically was

$$\rho_0 R\ddot{R} + (3/2)\rho_0 \dot{R}^2 = p_{g0}(R_0/R)^{3\kappa} + p_v - p_{L0} - 2\sigma/R - \delta_t \omega \rho_0 R\dot{R} - p(t), \tag{1}$$

where

$$p_{g0} = 2\sigma/R_0 + p_{L0} - p_v. \tag{2}$$

The symbols have the following meanings: R is the radius of the bubble at time t, and R_0 is the initial radius, ρ_0 is the density of the surrounding liquid, p_{g0} is the initial gas pressure inside the bubble, κ is the polytropic exponent of gas, p_v is the vapor pressure, p_{L0} is the hydrostatic pressure, σ is the surface tension coefficient, $p(t)$ is the time-varying pressure, ω is its angular frequency, and δ_t is the total damping coefficient.

The equation differed from that studied by Lauterborn[25] in the use of a total damping coefficient which included viscous, thermal, and acoustic damping as the sum

$$\delta_t = \delta_\mu + \delta_{ac} + \delta_{th}. \tag{3}$$

The viscous, acoustic, and thermal damping coefficients were given by

$$\delta_\mu = 4\mu/(\omega \rho_0 R_0^2), \tag{4}$$

$$\delta_{ac} = (\omega R_0/c)[1 + (\omega R_0/c)^2]^{-1}, \tag{5}$$

and

$$\delta_{th} = (\omega_0/\omega)^2 B. \tag{6}$$

TABLE I. Parameters of the model.

Hydrostatic pressure	p_{L0}	101 kPa
Density of water	ρ_0	998 kg m^{-3}
Vapor pressure	p_v	2.33 kPa
Coefficient of surface tension	σ	0.0725 N m^{-1}

In these equations, c is the speed of sound in the liquid and B is the thermal damping contant of Prosperetti.[28] Lauterborn included only the effects of viscous damping, but two of the three bubble sizes he studied (0.1, 1.0, and 10.0 μm) were small enough that these effects were dominant.[25] The assumption that only viscous damping was significant would not have been valid for most of the cases studied here.

The derivations for these expressions for the damping constants have been based on linear treatments,[24,26,28,43] so for very large amplitude oscillations these expressions may not be appropriate. For the conditions of interest in these investigations, however, which involved relatively small departures from linearity, they should be reasonable.

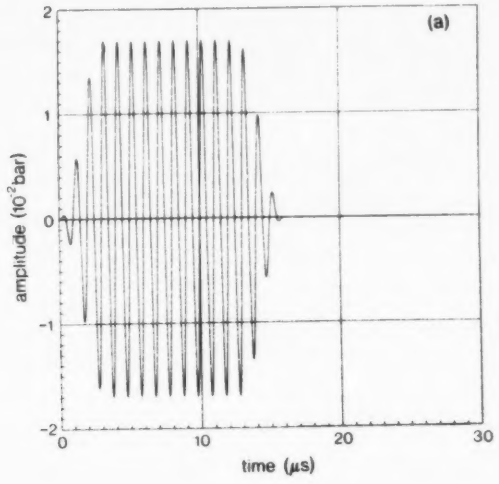

FIG. 1. (a) An example of a waveform used to excite bubbles in the numerical simulation—frequency, 1 MHz, duration 16 μs. A 40% cosine taper was applied to the pulse. (b) The periodogram of the waveform shown in (a).

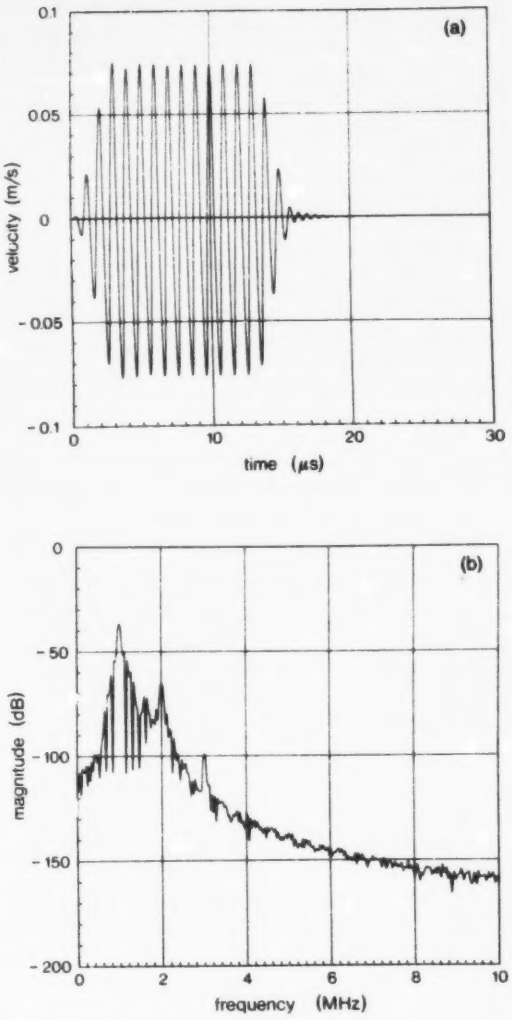

FIG. 2. (a) The radial velocity response of a bubble of radius 2 μm to the waveform in Fig. 1. (b) The periodogram of the response in (a).

The value assigned to the polytropic exponent was, in most cases, that of Prosperetti[28] for the appropriate conditions of bubble radius and driving frequency. In previous studies, this parameter has usually been set to a value in the range 1.0 to 1.4, corresponding to the isothermal and adiabatic conditions. For example, Lauterborn chose a value of 1.33. Recently, Crum[44] has provided experimental support for the predictions of Prosperetti[28] and Eller,[29] but warns that their models are less accurate for resonant bubbles.

Cramer and Lauterborn[35] have extended Lauterborn's[25] numerical analysis using the model of Gilmore (as described by Cramer and Lauterborn[35,36] and Flynn[31]), which includes compressibility of the liquid, and therefore the damping effect of acoustic radiation, directly. This more elaborate model is needed when the radial velocity of the bubble wall approaches the speed of sound. With this model they studied oscillations of bubbles with resting radii of 10 μm and larger. Their results show that for low amplitudes the bubble wall velocity remains small compared to the

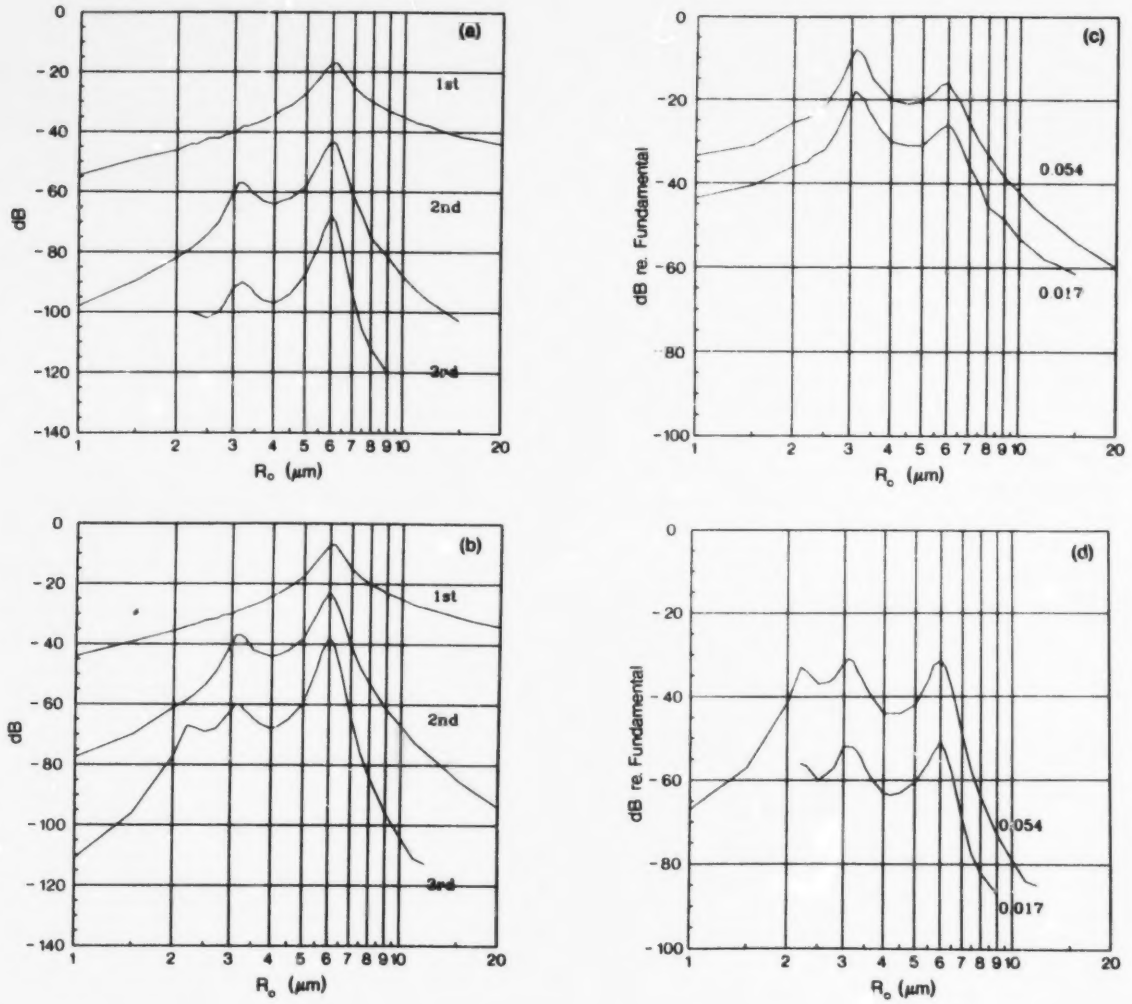

FIG. 3. (a) First, second, and third harmonic levels of bubble radial velocity, as a function of bubble radius, for pulsed ultrasound of frequency 500 kHz, pulse width 32 μs, and amplitude 0.017 bar. (b) As in (a), but for amplitude 0.054 bar. (c) The level of the second harmonic component, relative to the fundamental, for amplitude 0.017 and 0.054 bar. (d) The level of the third harmonic component, relative to the fundamental, for amplitudes 0.017 and 0.054 bar.

speed of sound. The "Rayleigh" model is therefore appropriate for the cases studied here.

The solution for the radial motion of the bubble in the time domain can be transformed into the frequency domain, to examine the corresponding spectral components. To determine the relative importance of these components in the scattered wave, the bubble may be modeled as a superposition of simple sources, each radiating at one of the frequencies in the autospectrum of the bubble's motion. The pressure radiated by a small simple source is proportional to its surface velocity and frequency.[45] Therefore, in many of the examples which follow, the surface velocity, rather than the surface displacement, has been plotted. It is assumed that the amplitude of the scattered waves is small enough that there would be no further changes in the spectrum caused by the nonlinearity of propagation.

II. METHODS

The parameters of the model were selected as appropriate for a bubble in water at 1 bar and 20 °C. Those which were constant are listed in Table I.

The initial conditions were usually those of a bubble at rest at its equilibrium radius, which was specified at run time. The "ultrasonic" excitation was of the form

$$p(t) = Af(t)\cos(\omega t + \phi), \tag{7}$$

where

$$f(t) = \begin{cases} 0.5 - 0.5\cos(\pi t/t_m), & 0 \leqslant t \leqslant t_m, \\ 1.0, & t_m < t < t_f - t_m, \\ 0.5 - 0.5\cos[\pi(t_f - t)/t_m], & t_f - t_m \leqslant t \leqslant t_f. \end{cases} \tag{8}$$

Here, t_f was the width of the pulse, and t_m was defined as a percentage of t_f, both specified at run time. The purpose of $f(t)$ was to vary the envelope of the ultrasonic pulse, to simulate pulses from real transducers. The parameter A was the amplitude of the ultrasound in bars, ϕ was the phase, normally set to $\pi/2$, and ω was the angular frequency.

The solution was obtained as both radial velocity and

radius versus time. Either the radial velocity or radius vector could then be passed to a fast-Fourier transform (FFT) program, to calculate the periodogram, which may be considered a raw estimate of the power spectral density of the signal.[46] The maximum size of the vector which could be handled by the FFT program was 1024 points. Since, in order to obtain sufficient accuracy, the time-domain vector was frequently longer than this, it was reduced to 1024 by taking equally spaced samples. A cosine taper, such as Eq. (8), was applied to the solution, before calculation of the FFT, to reduce errors caused by truncation of the time series.

Figure 1 is an example of a driving pulse showing the cosine-tapered envelope. The periodogram of this pulse is also displayed. Figure 2 shows the response of a bubble of radius 2 μm to the pulse in Fig. 1. The periodogram provides only relative information about the levels of the harmonics, because the calculated magnitude is dependent on the pulse duration, the width of the time window, and the length of the cosine taper used. In this example, the second harmonic of the radial velocity is 30 dB below, and the third harmonic is 63 dB below the fundamental. Because of the frequency dependence of the radiated pressure, these levels would be 24 and 54.5 dB below the fundamental for a pressure-sensitive transducer.

Various cases were studied numerically. The earliest investigations concerned bubbles of 50-μm radius, because this radius was about the smallest which could be produced by forcing gas through an orifice. Solutions were obtained for various combinations of driving frequency, amplitude, and pulse shape. Also, parameters such as the damping constant and the polytropic exponent were varied to assess the sensitivity of the results to differences in the estimates of these quantities. Since most ultrasonic instruments operate at a single frequency, a survey of the bubble spectra for bubbles of different radii was carried out for conditions of constant frequency and pulse shape. Finally, to check the validity of the results, comparisons were made with the numerical and analytical results of Lauterborn,[25] Nishi,[34] and Zabolotskaya and Soluyan.[39]

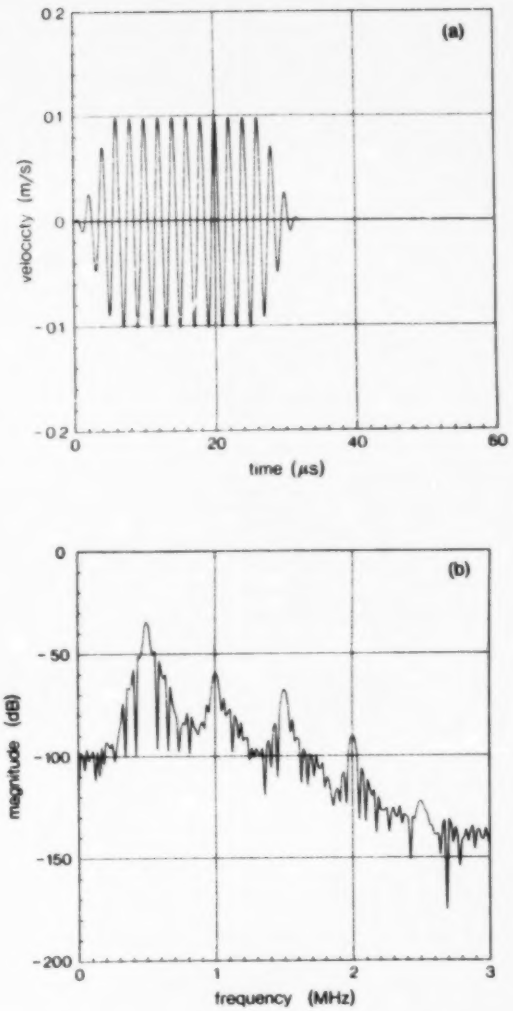

FIG. 4 (a) The radial velocity response of a bubble of radius 2.2 μm to a pulse of ultrasound of frequency 500 kHz, width 32 μs, and amplitude 0.054 bar. (b) The periodogram of the response in (a).

III. RESULTS

A. Variation of bubble size for fixed frequency, amplitude, and pulse duration

The frequency, amplitude, and pulse duration were fixed, while bubble size was varied, to determine what population of bubbles would contribute significantly to the harmonic signals. The study was carried out for two frequencies, 1 MHz and 500 kHz, and for two amplitudes at each frequency, 0.017 and 0.054 bar. For the pulses with a carrier frequency of 1 MHz, the duration was 16 μs, as in Fig. 1. For the 500-kHz pulses, the duration was 32 μs. The frequency of 1 MHz represents the lower end of the range typically used in biomedical ultrasonics, but the frequency 500 kHz may be more useful for bubble detection. Lower frequencies become more inconvenient because larger transducers are required. The amplitudes correspond to plane wave intensities of 10 and 100 mW cm^{-2}, respectively, which are representative of low-power, diagnostic medical instruments.

For brevity, only the 500-kHz results are shown here. The results for 1 MHz are similar but shifted towards smaller bubble radii.[43] Figure 3(a) shows the fundamental, second, and third harmonic components as obtained from the bubble velocity periodograms for the amplitude 0.017 bar. Figure 3(b) shows the results for 0.054 bar. At each discrete bubble radius, new values of κ and δ_t were used by referring to Prosperetti.[28] Plots of the ratio of the second and third harmonics to the fundamental for both amplitudes are shown in Fig. 3(c) and (d).

From Fig. 3 it is apparent that the bubbles that contribute significantly to the nonlinear scattering at 500 kHz are less than 8 μm in radius. Although all harmonic components exhibit absolute maxima for bubbles of resonance size (6 μm), the relative importance of the second harmonic is greatest for bubbles one-half this radius. The third harmonic exhibits peaks for bubbles of resonance size, one-half, and one-third resonance size.

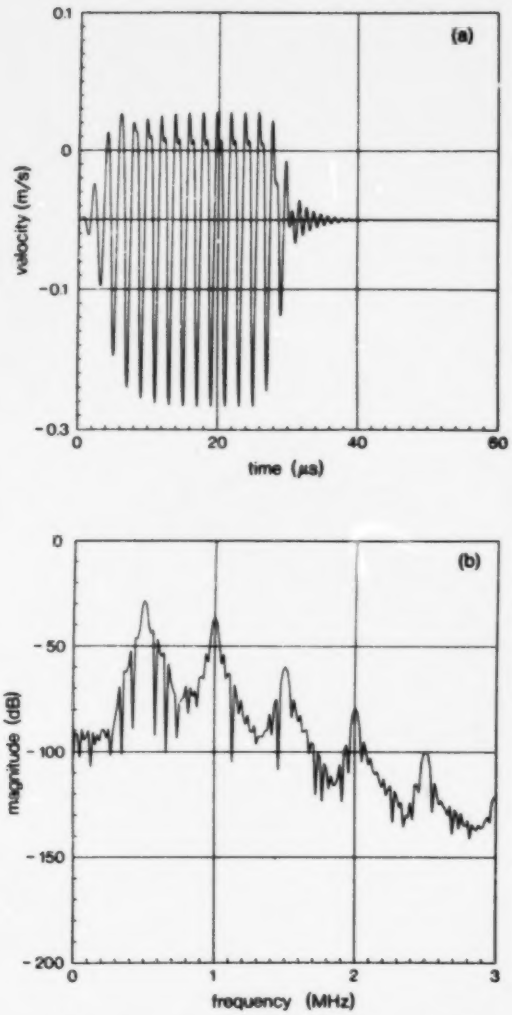

FIG. 5. (a) The radial velocity response of a bubble of radius 3.2 μm to a pulse of ultrasound of frequency 500 kHz, width 32 μs, and amplitude 0.054 bar. (b) The periodogram of the response in (a).

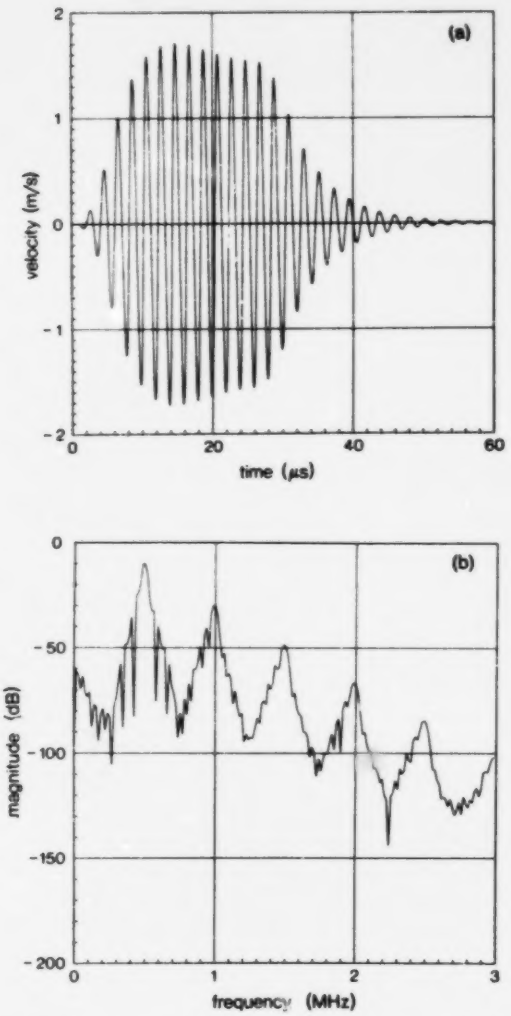

FIG. 6. (a) The radial velocity response of a bubble of radius 6.5 μm to a pulse of ultrasound of frequency 500 kHz, width 32 μs, and amplitude of 0.054 bar. (b) The periodogram of the response in (a).

Figures 4–7 show plots of the radial velocity in the time and frequency domains, for four bubble sizes of interest. The waveform in Fig. 4, showing the response for a bubble of radius 2.2 μm, appears to be relatively undistorted, even though this represents a maximum for the ratio of the third harmonic to the fundamental. In contrast, the response for a bubble of radius 3.2 μm, shown in Fig. 5, appears flattened. This represents a maximum in the ratio of second harmonic to fundamental components. In Fig. 6, resonance is evident in the long time taken for the response to grow and decay. Finally, Fig. 7 shows the response of a bubble larger than resonance size. The periodogram exhibits an asymmetry towards lower frequencies, indicating that the natural frequency of the bubble is less than the driving frequency. Although the reverse is true for bubbles smaller than resonance size, the effect is less noticeable.

B. Effect of varying δ_t and κ near resonance

To determine the sensitivity of the results to different values of the damping constant and the polytropic exponent, these parameters were varied while others were held constant. Figure 8 shows the level of the fundamental component, and the levels of the second and third harmonic components relative to the fundamental for values of the damping constant varying from 0 to 1.0. The case illustrated is for a bubble of radius 50 μm, driven by a pulse with center frequency 65 kHz and amplitude 0.1 bar. The theoretically predicted value[34] of the damping constant, 0.096, lies in the area where the curves are changing rapidly. This predicts that the nonlinearity of the response is sensitive to this parameter.

The main effect of varying the polytropic exponent κ was to shift the resonance frequency, which, if damping is neglected, is given by[33]

$$\omega_0^2 = 3\kappa p_{g0}(1 + 2\sigma/p_{g0}R_0)/(\rho_0 R_0^2) - 2\sigma/\rho_0 R_0^3. \quad (9)$$

The nonlinearity of the response, as indicated by the ratio of second harmonic to fundamental components in Table II, was not much altered, especially when the driving frequency was allowed to track the resonance frequency.

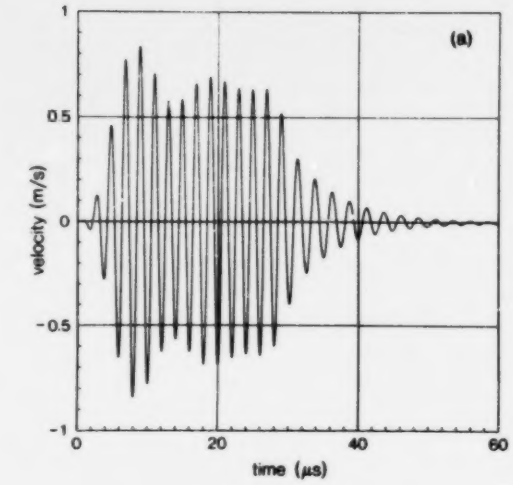

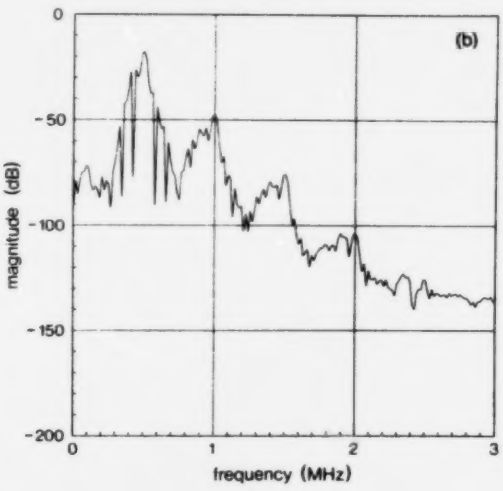

FIG. 7. (a) The radial velocity response of a bubble of radius 7.5 μm to a pulse of ultrasound of frequency 500 kHz, width 32 μs, and amplitude 0.054 bar. (b) The periodogram of the response in (a).

C. Driving frequency much greater than resonance frequency

For ultrasonic frequencies 16 times greater than the resonance frequency of the bubble, the second harmonic component was more than 70 dB below the fundamental for amplitudes up to 1.2 bar. By any practical definition, therefore, the bubble was behaving linearly.

When the driving frequency had been reduced to twice the resonance frequency, the nonlinearity became noticeable. For example, for a bubble of radius 50 μm, driven at a frequency of 128 kHz, and amplitude of 0.2 bar, the second harmonic was 35 dB below the fundamental.

For frequencies far above resonance, one effect of the bubble response was evident. The lower frequency components were increased at the expense of the higher frequency components, when compared with the periodogram of the driving pulse. This was an effect of the transient resonant oscillation excited by the pulse, which appeared as a modulation of the response at the driving frequency. The effect, illustrated in Fig. 9, was especially noticeable for sharp pulses. In Fig. 9(a) and (b), an excitation pulse of frequency 500 kHz, width 16 μs, amplitude 0.05 bar, and taper 10% is shown along with its periodogram. The calculated response of a bubble, of radius 50 μm, to the driving pulse in 9(a) is shown in 9(c), and its periodogram is shown in 9(d). It can be seen that the lower frequency components are emphasized, particularly in the neighborhood of the resonance frequency.

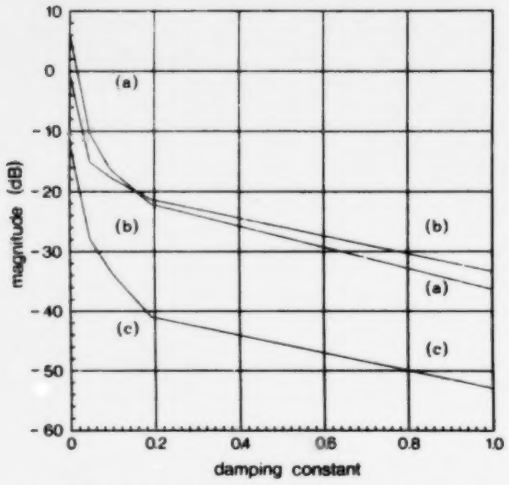

FIG. 8. A plot showing the effect of altering the damping constant on the nonlinearity of the response of a bubble of radius 50 μm, driven at resonance. (a) The fundamental component of the radial velocity. (b) The second harmonic relative to the fundamental. (c) The third harmonic relative to the fundamental.

D. Driving frequency much less than resonance frequency

Figure 3 showed that distortion levels remained high as the bubble size was reduced below resonance size. For bubbles of radius ranging from 2–5 μm, with a driving frequency of 100 kHz (ratio of driving frequency to resonance frequency varying from 0.059 to 0.165), the ratio of second harmonic to fundamental components of the radial velocity varied from -32 to -29 dB, for a pulse amplitude of 0.054 bar, and from -42 to -39 dB for an amplitude of 0.017 bar. These conditions represent the lowest frequency and smallest bubble size which might be of interest for bubble detection *in vivo*.

TABLE II. The effect of the polytropic exponent on bubble nonlinearity. In this table, κ is the polytropic exponent, f is the driving ultrasonic frequency; f_r is the linear resonance frequency of the bubble; U_1 is the fundamental component of the bubble's radial velocity, in dB *re*: 1 m s^{-1}, and U_2 and U_3 refer to the second and third harmonic components, respectively.

κ	f (kHz)	f_r (kHz)	U_1 (dB)	U_2/U_1 (dB)	U_3/U_1 (dB)
1.40	65.0	65.6	−16.2	−17.5	−33.2
1.33	65.0	64.0	−16.3	−18.0	−33.8
1.22	65.0	61.3	−19.9	−19.8	−37.5
1.22	61.3	61.3	−16.1	−17.4	−31.7

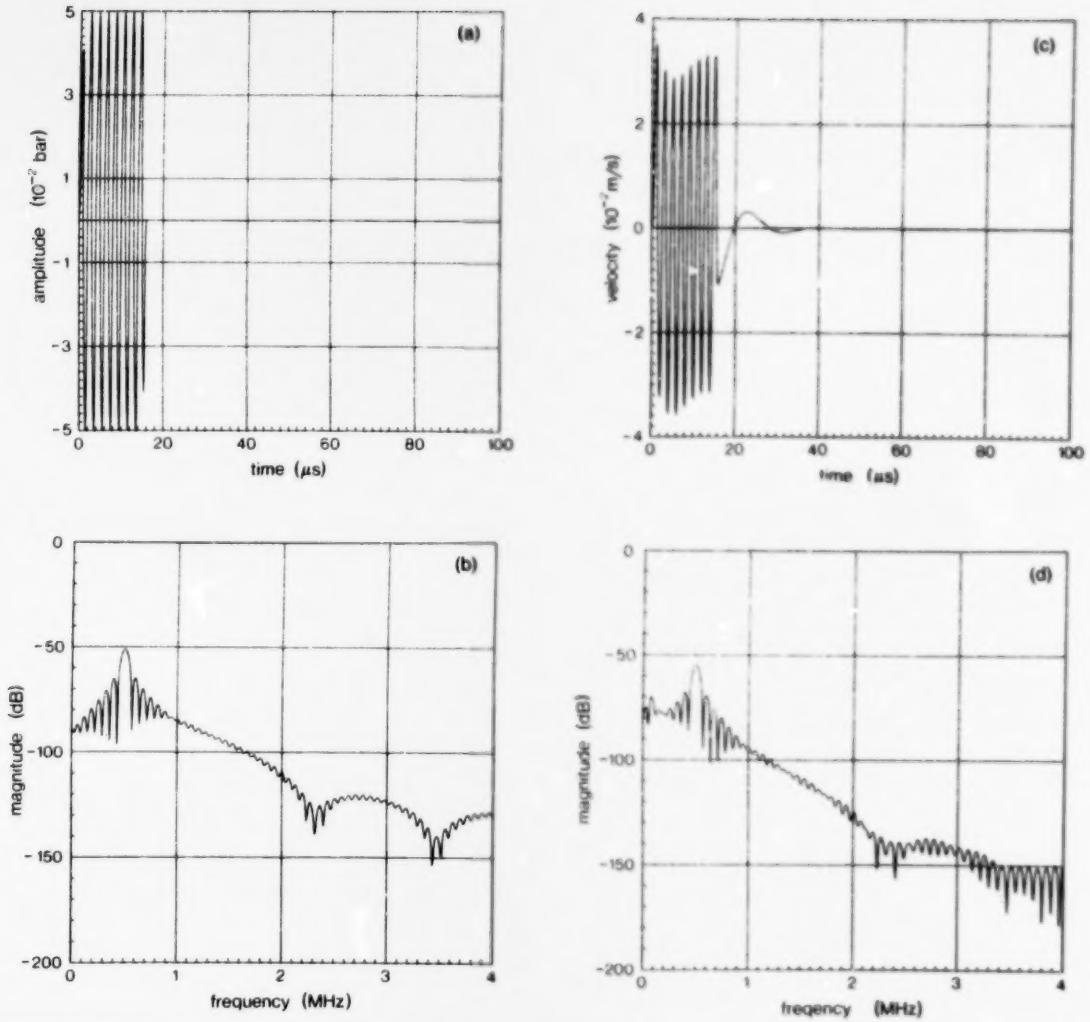

FIG. 9. (a) A numerical excitation pulse, of frequency 500 kHz, width 16 μs, amplitude 0.05 bar, and taper 10%. (b) The periodogram of the pulse in (a). (c) The calculated response of a bubble of radius 50 μm to the pulse shown in (a). (d) The periodogram of the response of the bubble, showing the emphasis of low-frequency components—an effect of the bubble's transient response.

E. Comparison with results available in the literature

As a check of the validity of the results, comparisons were made with some results published by Lauterborn,[25] Nishi,[34] and Zabolotskaya and Soluyan.[39]

Lauterborn[25] showed a radius-time curve and power spectrum for the case of a bubble of radius 10 μm driven by a continuous sinusoidal wave of frequency 646.6 kHz and amplitude 0.7 bar. His solution for this case exhibited a subharmonic response. In this study, with what are presumed to be the same conditions, a "subharmonic" response was also obtained,[43] in agreement with Lauterborn.

Calculations of the scattered intensity by bubbles of radius 1 and 10 μm in ultrasound of frequency 5 MHz and amplitude 0.1 bar, at a distance of 1 cm from the bubble agreed very well with Nishi's[34] plotted results.

The expression of Zabolotskaya and Soluyan[39] for the second harmonic of the bubble volume oscillations agreed well with the numerical results in some instances, but differed by as much as 11 dB in others. For example, their expression predicted a response smaller by 1.27 dB for a 50-μm radius bubble driven at 55 kHz at 0.054 bar, but 9 dB larger when the same bubble was driven at 65 kHz.[43]

F. Effect of tapering the driving waveform

When solving for continuous wave excitation at higher amplitudes (e.g., 0.7 bar), a large number of periods may be required before the bubble oscillations reach a steady state. This is analogous to a turn-on transient, but its effect is amplified by the nonlinearity of the system. It was observed that the time to reach the steady state could be reduced by using an appropriate cosine taper on the driving waveform. When this was done, the final form of the oscillations was the same, despite the nonlinearity of the system.

G. Free oscillations

Free oscillations of a gas bubble, such as might occur when a bubble experiences an initial perturbation in radius,

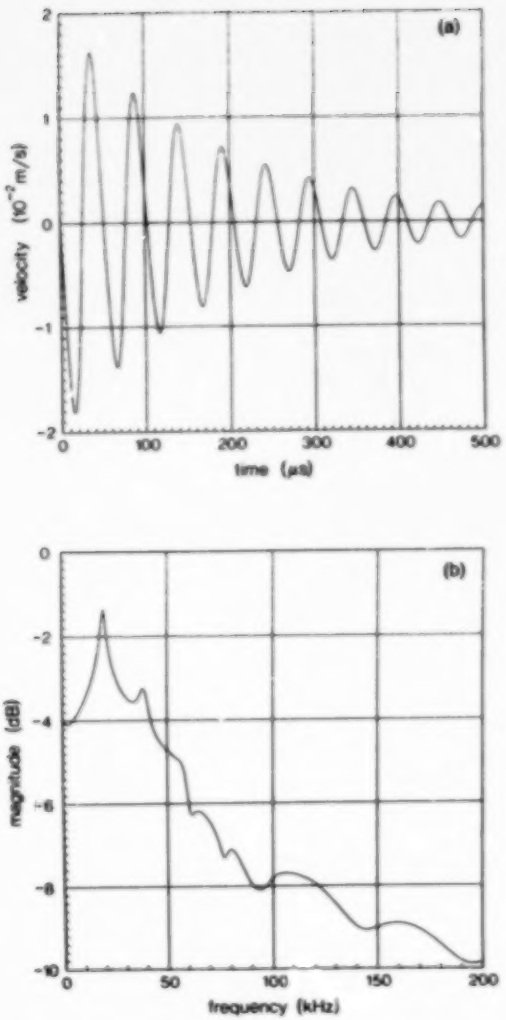

FIG. 10. (a) A numerical result showing the response of a bubble with an initial radial displacement of + 10% of its equilibrium radius, 161 μm. (b) The periodogram of the response shown in (a).

were simulated by setting the amplitude of the driving pressure to zero, and setting the initial radius different from the equilibrium radius. An example of a solution obtained for a bubble of equilibrium radius 161 μm, with an initial radial displacement of + 10% is shown in Fig. 10. When a bubble is formed, it may grow large enough so that buoyancy overcomes surface tension and it breaks free of its formation site (e.g., an orifice or crevice). This initial perturbation sets up free oscillations, which, though not purely radial, nevertheless have a strong radial component.[43]

IV. DISCUSSION

These studies have shown that the behavior of bubbles in an ultrasonic field of low to moderate amplitude (0.01 to 1 bar) is essentially linear, unless the driving frequency matches one of the following conditions: it is within 10% of the radial resonance frequency of the bubble, or it is a low integer fraction (1/2, 1/3,...) of the resonance frequency, or, to a lesser extent, it is a low harmonic of the resonance frequency. The maximum of the ratio of the second harmonic component to the fundamental occurs when the driving frequency was one-half of the radial resonance frequency. All harmonics exhibit absolute maxima at the resonance frequency.

These results imply that low power ultrasonic bubble detection techniques, which exploit the nonlinearity of the bubble's response, will be sensitive only to certain populations of bubbles. Figure 3 shows, for example, that for a driving frequency of 500 kHz, only bubbles less than about 8 μm in radius would be detected, preferentially those of radius 3 and 6 μm. Current methods of bubble detection in humans detect bubbles considerably larger than this, but the actual distribution of bubble sizes in tissue is not known.

Tapered, pulsed, ultrasonic excitation was used for most of the cases studied here. It was observed that the transient oscillations which form part of the bubble's response to pulsed ultrasound, appear as discrete spectral components, near the resonance frequency, if the driving and resonance frequencies are widely separated. Otherwise, the transient oscillations produce an elevation in the spectrum towards the resonance frequency. Observations of these characteristics in the spectra of scattered pulses might permit an estimation of bubble size. Sweeping the ultrasonic frequency could also yield an estimate of bubble size.[34] However, the range of bubble sizes would be restricted to less than about 30 μm in radius, because of practical limitations on the range of ultrasonic frequencies that could be swept.

If the process of bubble formation *in vivo*, involves growth of the bubble in a crevice[47,48] followed by release into the blood when the bubble grows large enough, then free oscillations of the bubble could occur. It might be possible to detect these oscillations passively with a sensitive, broadband transducer, similar to those used to detect acoustic emissions in nondestructive testing, but probably of lower frequency.

The use of a cosine-tapered driving waveform was found to reduce the time taken to reach steady state for continuous-wave excitation, and the steady state was not noticeably different from the untapered case. This could be of practical use in obtaining numerical solutions. It also represents a more realistic waveform, since abrupt transitions (either temporal or spatial) are difficult to achieve, especially with resonant devices.

For these numerical studies, the best available estimates of the damping constants and polytropic exponents were used. The nonlinearity of the response was sensitive to the damping constant for values close to, or less than, the predicted damping constant. For moderate ultrasonic amplitudes, the nonlinearity was not sensitive to variation of the polytropic exponent. For amplitudes around 0.5 bar or more, the nature of the response was sensitive to these values.[43] Since these constants were predicted using linear theories, it may be that for higher amplitudes a more accurate approach is needed.

V. CONCLUSION

Numerical studies of Rayleigh's equation for the motion of bubbles in an ultrasonic field have shown the condi-

tions for which appreciable nonlinearity could be observed in the bubble's response, given low to moderate ultrasonic amplitudes. The application of the nonlinear effect to the detection of bubbles would be limited to bubbles of small size, ordinarily, less than 10 μm in radius. Primarily, bubbles of one-half resonance size and resonance size would be detected by this technique.

[1]D. J. Kidd and D. H. Elliott, "Decompression disorders in divers," in *The Physiology and Medicine of Diving and Compressed Air Work*, edited by P. B. Bennett and D. H. Elliott (Baillière Tindall, London, 1975), 2nd ed., Chap. 25, pp. 471–495.

[2]*Decompression of Compressed Air Workers in Civil Engineering*, edited by R. I. McCallum (Oriel, Newcastle upon Tyne, 1967).

[3]D. I. Fryer, *Subatmospheric Decompression Sickness in Man* (Technivision Services, Slough, England, 1969).

[4]*Dysbarism-related Osteonecrosis. Proceedings of a Symposium on Dysbaric Osteonecrosis* (U.S. Dept. H.E.W., Washington, DC, 1974).

[5]A. Evans, "Ultrasonic surveillance of decompression," in *The Physiology and Medicine of Diving and Compressed Air Work*, edited by P. B. Bennett and D. H. Elliott (Baillière Tindall, London, 1975), 2nd ed., Chap. 22, pp. 417–434.

[6]*The Twelfth Undersea Medical Society Workshop on Early Diagnosis of Decompression Sickness*, edited by R. Pearson (Undersea Medical Society Inc., Bethesda, MD, 1977).

[7]R. Y. Nishi, K. E. Kisman, B. C. Eatock, I. P. Buckingham, and G. Masurel, "Assessment of decompression profiles and divers by Doppler ultrasonic monitoring," in *Underwater Physiology VII: Proceedings of the Seventh Symposium on Underwater Physiology*, edited by A. J. Bachrach and M. M. Matzen (Undersea Medical Society Inc., Bethesda, MD, 1981), pp. 717–727.

[8]G. J. Rubissow and R. S. Mackay, "Ultrasonic imaging of *in vivo* bubbles in decompression sickness," Ultrasonics **9**, 225–234 (1971).

[9]S. Daniels, W. D. Paton, and E. B. Smith, "Ultrasonic imaging system for the study of decompression-induced bubbles," Undersea Biomed. Res. **6**, 197–207 (1979).

[10]R. Y. Nishi, "Ultrasonic detection of bubbles with Doppler flow transducers," Ultrasonics **10**, 173–179 (1972).

[11]J.-L. Monjaret, R. Guillerm, and G. Masurel, "Detecteur ultrasonre à effet Doppler de bulles circulantes dans les vaisseaux sanquins," in *Colloque international sur les capteurs bio-médicaux, Biocapt 75* (Comité d'organisation du colloque international sur les capteurs bio-médicaux, Paris, 1975), pp. 93–98.

[12]T. W. Beck, S. Daniels, W. D. M. Paton, and E. B. Smith, "Detection of bubbles in decompression sickness," Nature **276**, 173–174 (1978).

[13]H. Moulinier, *Détection de Bulles dans les Tissus Biologiques par Mesure de Taux de Distortion d'une Onde Ultrasonore*, doctoral thesis, L'Institute National des Sciences Appliquées de Lyon (1978).

[14]D. L. Miller, "Ultrasonic detection of resonant bubbles by their second harmonic emissions," J. Acoust. Soc. Am. Suppl. 1 **69**, S26 (1981).

[15]D. L. Miller, "Ultrasonic detection of resonant cavitation bubbles in a flow tube by their second harmonic emissions," Ultrasonics **19**, 217–224 (1981).

[16]D. L. Storm, "Frequency spectrum of finite-amplitude radiation from the non-linear pulsation of a gas bubble," Ph.D. thesis, University of Vermont (1975).

[17]Lord Rayleigh, "On the pressure developed by a liquid during the collapse of a spherical cavity," Philos. Mag. **34**, 94–98 (1917).

[18]M. S. Plesset, "The dynamics of cavitation bubbles," J. Appl. Mech. **16**, 272–282 (1949).

[19]B. E. Noltingk and E. A. Neppiras, "Cavitation produced by ultrasonics," Proc. Phys. Soc. **63B**, 674–685 (1950).

[20]H. Poritsky, "The collapse or growth of a spherical bubble or cavity in a viscous fluid," in *Proceedings of the First U.S. National Congress on Applied Mechanics*, edited by E. S ernberg (American Society of Mechanical Engineers, New York, 1952), pp. 813–821.

[21]W. Lauterborn, "Numerical investigations of nonlinear oscillations of gas bubbles in liquids," J. Acoust. Soc. Am. **59**, 283–293 (1976).

[22]F. Smith, "On the destructive mechanical effects of gas bubbles liberated by the passage of intense sound through a liquid," Philos. Mag. **19**, 1147–1151 (1935).

[23]C. Devin, Jr., "Survey of thermal, radiation, and viscous damping of pulsating air bubbles in water," J. Acoust. Soc. Am. **31**, 1654–1667 (1959).

[24]A. Prosperetti, "Thermal effects of damping mechanisms in the forced radial oscillations of gas bubbles in liquids," J. Acoust. Soc. Am. **61**, 17–27 (1977).

[25]A. I. Eller, "Damping constants of pulsating bubbles," J. Acoust. Soc. Am. **47**, 1469–1470 (1970).

[26]D. Y. Hsieh and M. S. Plesset, "Theory of the acoustic absorption by a gas bubble in a liquid," 85–19, Eng. Div., Caltech (1961).

[27]H. G. Flynn, "Physics of acoustic cavitation in liquids," in *Physical Acoustics*, edited by W. P. Mason (Academic, New York, 1964), pp. 57–172.

[28]O. A. Kapustina, "Gas bubble in a small-amplitude sound field," Akust. Zh. **15**, 489–504 (1969). [English transl.: Sov. Phys. Acoust. **15**, 427–438 (1970).]

[29]R. B. Chapman and M. S. Plesset, "Thermal effects in the free oscillations of gas bubbles," J. Basic Eng. **93**, 373–376 (1971).

[30]R. Y. Nishi, "The scattering and absorption of sound waves by a gas bubble in a viscous liquid," Acustica **33**, 173–179 (1975).

[31]E. Cramer and W. Lauterborn, "Zur dynamik und schallabstrahlung kugelförmiger kavitationsblasen in einem schallfeld," Acustica **49**, 226–238 (1981).

[32]E. Cramer, "The dynamics and acoustic emission of bubbles driven by a sound field," in *Cavitation and Inhomogeneities in Underwater Acoustics*, edited by W. Lauterborn (Springer-Verlag, Berlin, 1980), pp. 54–63.

[33]G. Gaunaurd, K. P. Scharnhorst, and H. Überall, "Giant monopole resonances in the scattering of waves from gas filled spherical cavities and bubbles," J. Acoust. Soc. Am. **65**, 573–594 (1979).

[34]G. C. Gaunaurd and H. Uberall, "Theory of resonant scattering from spherical cavities in elastic and viscoelastic media," J. Acoust. Soc. Am. **63**, 1699–1712 (1978).

[35]E. A. Zabolotskaya and S.I. Soluyan, "Emission of harmonic and combination frequency waves by air bubbles," Akust. Zh. **18**, 472–474 (1972). [English transl.: Sov. Phys. Acoust. **18**, 396–398 (1973).]

[40]A. Prosperetti, "Nonlinear oscillations of gas bubbles in liquids: Steady-state solutions," J. Acoust. Soc. Am. **56**, 878–885 (1974).

[41]A. Prosperetti, "Nonlinear oscillations of gas bubbles in liquids: Transient solutions and the connection between subharmonic signal and cavitation," J. Acoust. Soc. Am. **57**, 810–821 (1975).

[42]M. S. Plesset and A. Prosperetti, "Bubble dynamics and cavitation," in *Annual Review of Fluid Mechanics*, edited by M. Van Dyke, J. V. Wehausen, and J. L. Lumley (Annual Reviews Inc., Palo Alto, CA, 1977), pp. 145–185.

[43]B. C. Eatock, "Nonlinear scattering of ultrasound by bubbles: Numerical and experimental investigations with application to their detection," Ph.D. thesis, University of Toronto (1981); UTIAS Rep. No. 261 (February 1982).

[44]L. A. Crum, "The polytropic exponent of gas contained within air bubbles pulsating in a liquid," J. Acoust. Soc. Am. **73**, 116–120 (1983).

[45]L. E. Kinsler and A. R. Frey, *Fundamentals of Acoustics* (Wiley, New York, 1962), 2nd ed., p. 164.

[46]A. V. Oppenheim and R. W. Schafer, *Digital Signal Processing* (Prentice-Hall, Engelwood Cliffs, NJ, 1975), p. 542.

[47]E. N. Harvey, D. K. Barnes, U. D. McElroy, A. H. Whitely, D. C. Pease, and K. W. Cooper, "Bubble formation in animals," J. Cell Comp. Physiol. **24**, 1–22 (1944).

[48]L. A. Crum, "Nucleation and stabilization of microbubbles in liquids," Appl. Sci. Res. **38**, 101–115 (1982).